ELSEVIER

Polymer 43 (2002) 1877–1886

polymer

www.elsevier.com/locate/polymer

On the effect of the nature of the side chain over the crystalline structure in aliphatic polyketones

J.M. Lagaron[1,a,*], M.E. Vickers[b], A.K. Powell[c], J.G. Bonner[c]

[a]*Department of Technology, Area of Materials, Universitat Jaume I, Campus Riu Sec, Castellon 12071, Spain*
[b]*Department of Materials Science and Metallurgy, University of Cambridge, Pembroke Street, Cambridge CB2 3QZ, UK*
[c]*BP Chemicals, Applied Technology, P.O. Box 21, Grangemouth, Stirlingshire FK3 9XH, UK*

Received 27 March 2001; accepted 29 November 2001

Abstract

The crystalline structure of a number of random polymers of perfectly alternating l-olefins/carbon monoxide aliphatic polyketones has been studied by wide angle X-ray scattering (WAXS), small-angle X-ray scattering (SAXS), differential scanning calorimetry (DSC) and Raman spectroscopy. From previous studies, WAXS, Raman and DSC have shown to be suitable techniques for the characterisation of the two crystalline polymorphs, α (denser) and β, detected in ethene/carbon monoxide (ECO) and in ethene/propene/carbon monoxide (EPCO) polymers. In this paper for the first time, polyketones with butene and hexene as the second olefin are reported. It was found that the ethene/propene/carbon monoxide polymers and ethene/butene/carbon monoxide (EBCO) polymers, predominately contain the β-rich crystalline phase. The crystalline density of this phase drops with increasing second olefin content, albeit at a faster pace for propene polymers. From the latter results, and from the behaviour of the melting point, crystallinity, and crystal thickness across composition, inclusion of methyl and ethyl side chains into the crystals as defects was inferred. Ethene/hexene/carbon monoxide (EHCO) polymers do seem to behave differently: they show lower crystallinity, the presence of a larger quantity of the denser α crystals and a relatively high and constant crystalline density for the β phase throughout composition; observations that unambiguously support the exclusion argument for the butyl branches. The above behaviour is surprising since for instance in polyethylene copolymers it is considered that only methyl branches can enter the crystal lattice. The relative presence of α crystals was found to decrease with increasing the concentration of branches and in the order EHCO > EBCO > EPCO.

Keywords: Aliphatic polyketones; X-ray; Raman spectroscopy

1. Introduction

Aliphatic polyketones are a family of polymers prepared by the polymerisation of olefins and carbon monoxide, in a perfectly alternating sequence, by means of palladium-based catalysts [1,2]. As a consequence, the mol-ratio olefins/carbon monoxide is one for all compositions. In order to produce polymers with varying melting points, a second olefin (propene, butene, etc.) is introduced in the polymerisation reaction substituting randomly for ethene. The introduction of the second olefin results in a tailor-made range of new materials with very attractive physical characteristics for commercial purpose. These semicrystalline thermoplastic materials have a unique combination of mechanical, high temperature, chemical resistance, wear and barrier properties. Aliphatic polyketones therefore have significant potential in a broad range of engineering, barrier packaging, fibre and blend applications [3,4].

The original structure that Chatany et al. [5,6] determined for aliphatic polyketones is directly analogous to the structure of polyethylene, space group *Pnam* (No. 62) but with *c* axis increased by three times to account for the carbonyl group. More recent work by Lommerts et al. [7] and Klop et al. [8] reported a denser phase. It had the same space group No. 62 but a different setting *Pbnm*. They designated this denser phase (density $\sim 1.39\ g\ cm^{-3}$) alpha (α) and the original structure characterized by Chatany (density $\sim 1.3\ g\ cm^{-3}$) beta (β). Both crystalline structures have two polymer chains in all trans conformation along the *c* axis, but differ in the mode of chain packing. The α form arises from a highly efficient dipolar intermolecular interactions within the lattice and has been reported to be in perfectly alternating polymers of ethylene and carbon

* Corresponding author. Tel.: +34-964-728-137; fax: +34-964-728-106.
E-mail addresses: lagaron@mail.uji.es (J.M. Lagaron).
[1] Present address: Institute of Agrochemistry and Food Technology, CSTC, Packaging Lab, Apdo Correos 73, 46100 Burjassot, Spain.

0032-3861/02/$ - see front matter
PII: S0032-3861(01)00787-X

monoxide with the amount increased by orientation. The less dense β form can accommodate more defects, both along the backbone and as side chains, as well as being the stable form at elevated temperatures before melting [8]. From a recent paper [9], cold-drawing of some EPCO polymers has been reported to promote the production of α crystals, in particular at low draw rate.

Raman spectroscopy characterisation of a range of EPCO ex-reactor aliphatic polyketones powders, revealed spectral differences in the $-CH_2-$ bending region [10]. These differences were attributed to factor group splitting arising from the different polymorphs described earlier. Hence, this technique proved to be very useful to rapidly characterise the crystalline polymorphism present in these polymers. Moreover, methodologies were provided to determine from the Raman spectrum other essential structural information, e.g. the propene incorporation, temperature-induced chemical changes, crystallinity content, etc. In this paper, the assignment of the weak differential scanning calorimetry (DSC) endotherms seen at around 100 °C (well below the polymer melting point) to solid–solid phase transformation from α to β phase was unambiguously proved. A further study [11] devoted to the study of the crystalline morphology of an ECO and a number of EPCO compression moulded samples by Raman, wide angle X-ray scattering (WAXS) and DSC techniques showed (i) an excellent agreement between the results drawn by the three different techniques and (ii) the α/β ratio followed trends similar to those reported by Klop et al. in Ref. [8]. Thus, while the ECO polymer was found to exhibit a mixture of α and β phase, EPCO polymers predominantly showed a β phase above 2.9 mol% of propene incorporation. Therefore, the ratio α/β is larger in ECO polymer and decreases rapidly with increasing second olefin content in propene polymers (EPCO). Moreover, other parameters like crystalline density, heat of fusion and melting point were seen to decrease with increasing propene level in the samples. The decrease in the crystalline density was principally caused by the enlargement of the *a* cell parameter of the orthorhombic lattice.

In the current study, we report and discuss the effects of varying the type and content of side chain (branching) on the crystalline morphology of a number of aliphatic polyketones as observed by WAXS, small-angle X-ray scattering (SAXS), Raman spectroscopy and DSC.

2. Experimental

2.1. Materials

The aliphatic polyketones, ECO, EPCO, EBCO and EHCO, used in this study were synthesized at BP Chemicals using a proprietary palladium-based catalyst. The materials were supplied in the powder form as obtained from the production process.

Films of 150 μm thickness were compression moulded at a temperature above the melting point, using an electrically heated hydraulic press and cooled under pressure at 15 °C min^{-1} to room temperature.

Sample codes are as follows: ECO is a perfectly alternating ethene/carbon monoxide polymer. EPCO is a perfectly alternating ethene/propene/CO polymer where the propene substitutes randomly for ethene. EBCO is a perfectly alternating ethene/butene/CO polymer where the butene substitutes randomly for ethene. EHCO is a perfectly alternating ethene/hexene/CO polymer where the hexene substitutes randomly for ethene.

The mol% of propene, butene and hexene as measured by ^1H NMR is given in parenthesis attached to the above codes throughout the paper. As an example, EPCO(2.9) designates a polymer comprising 2.9 mol% of propene, 47.1 mol% of ethene and 50 mol% of carbon monoxide. The weight average molecular weight (M_w) determined by gel permeation chromatography ranges from 105 000 to 200 000, albeit it is for most of the samples around 130 000, relative to PMMA standards and the polydispersity index is between 2.1 and 2.9.

2.2. Raman equipment

The spectra were recorded with a Raman system [12] comprising of JY THR1000 single monochromator, Wright instruments CCD camera, Ti sapphire laser at 752 nm, with a Kaiser holographic edge filter. Typically 50 mW of laser light was used at the sample with a ×20 long distance microscope objective. Integration times were around 20 s and the spectral resolution is 3 cm^{-1}.

2.3. Wide angle X-ray scattering

The X-ray data were obtained in a Bruker D500 diffractometer operating in reflection mode. The thin polymer films (~0.11–0.26 mm) were mounted on a single crystal silicon substrate cut to give no background scattering. The data were fitted, with pseudo-Voigt functions, using the Philips program PROFIT to determine peak positions, intensities, widths and integrated areas [13]. The peak positions were corrected for absorption into the sample by using the following formula by Vonk and Wilson [14,15].

$$\Delta 2\theta(\text{radians}) = -\frac{\sin 2\theta}{2\mu R} - \frac{2t\cos\theta}{R(e^{2\mu t \,\text{cosec}\,\theta} - 1)}$$

where R is the radius of the diffractometer, t, the sample thickness and μ, the linear absorption coefficient.

The cell parameters determined by a least squares fit to about 7–10 reflections using the Bruker program Appleman. Well-resolved reflections were given a high weighting and the very weak or poorly resolved ones a low weighting in the fitting procedure. In several instances there was a lack of strong reflections with an index of one, thus the value for the *c* cell parameter has not really been determined but rather allowed to refine using as input the literature value. Crystalline densities (ρ_c) have been calculated from the

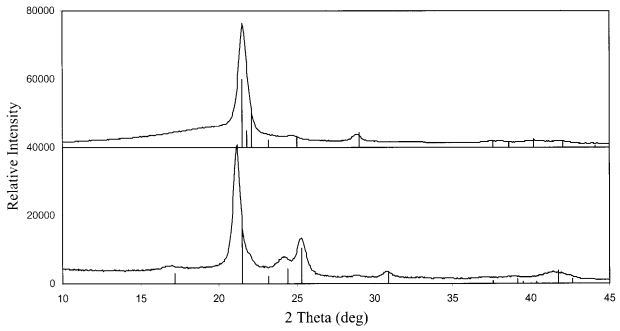

Fig. 1. WAXS patterns of a material showing mainly α phase (bottom) and of a material showing only β phase (top).

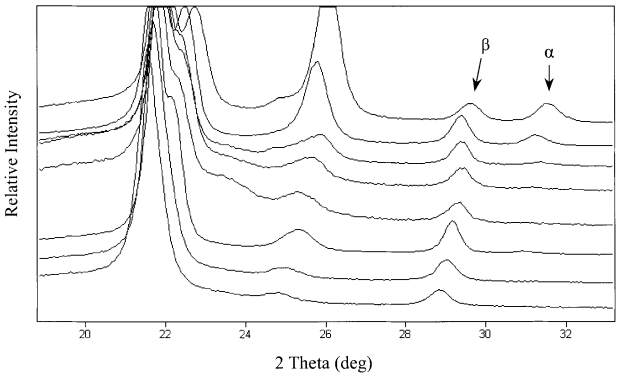

Fig. 2. WAXS curves of, from top to bottom, ECO, EPCO(1.2), EHCO(2.3), EHCO(4.8), EBCO(4.8), EPCO(2.9), EPCO(5.1), EPCO(7.2).

experimental cell parameters assuming that the unit cell contains just two polyketone chains.

2.4. Small-angle X-ray scattering

Data were collected in an automated step scanning Kratky camera with a Cu K_α X-ray source. The data were processed in a modified version of Vonk's program [16]. Values for the long period repeat obtained by applying Bragg's law to the maximum of the desmeared Lorentz corrected data and from the maximum of a one dimensional correlation function.

2.5. Differential scanning calorimetry

The DSC experiments were carried out in Perkin–Elmer DSC 7 calorimeter at a heating speed of 10 °C min^{-1} on typically 4 mg of sample cut from the same films used for WAXS measurements. The calibration of the DSC was carried out with a standard sample of tin.

3. Results

3.1. Crystalline polymorphism

Fig. 1 shows the WAXS patterns of two extreme samples in terms of polymorphism, the bottom curve shows a high content of α phase, whereas the top curve shows predominantly β phase peaks [11]. A comprehensive description of the WAXS peak assignments and of modelling work leading to the characterisation of the two-polymorph lattices is given in Refs. [5–8]. The peaks at 29 and 31° relate to the (210) reflection of the β and α phases, respectively. Because they are well resolved, they have been used for phase identification as well as to quantify the ratio of these phases [11]. The WAXS data of a number of polyketone samples varying in second olefin type and content are shown in Fig. 2. The major differences among the WAXS patterns of the samples arise form variations in the ratio of α to β. Fig. 1 shows that the peak at 31° assigned to the α phase crystals has the largest intensity for the ECO sample closely followed by EPCO(1.2). This peak is also clearly present in the EHCO materials measured. On the other hand, in the EBCO(4.8) sample and in the other EPCO materials (above 1.2 mol% of propene) this reflection is very weak or not at all present. Table 1 shows the WAXS peak are ratio 31°/29° for the different samples. The relative intensities of the latter peaks were used to calculate weight fractions of each phase (see Table 1). The calibration can be performed by making up standards of known content or calculating the X-ray data

Table 1
Area ratio of (210) reflections 31°/29°, %α phase in the crystalline fraction from the (210) reflections and in parenthesis by Rietveld, the heat change associated with the solid–solid phase transition, the estimated enthalpy for the perfect crystal (H_f) using as input WAXS crystallinity, and the Raman α phase $-CH_2-$ bending splitting separation

Sample	WAXS		$H_{\alpha\rightarrow\beta}$ (J g^{-1})	H_f (J g^{-1})	$-CH_2-$ bending splitting (cm^{-1})
	α/β	% α			
ECO	1.13	53 (45–55)	11.6	196.4	25
EPCO(1.2)	0.43	30	5.8	149.8	24
EPCO(2.9)	0.08	8	–	132.5	–
EPCO(5.1)	<0.01	<1	–	132.2	–
EPCO(7.2)	0	0	–	146.2	–
EBCO(4.8)	0	0	–	151.7	–
EHCO(2.3)	0.22	18	3.4	168.7	24
EHCO(4.8)	0.09	8 (5–15)	1.5	157.0	22

from known structures and determining the ratio of the scale factors say be Rietveld refinement. Here, the ratio of the (210) reflection to the strongest interchain scattering peak was calculated from data in the literature giving a value of 0.145, from (210)/(110), for the α phase. For the β phase, (210)/(110) + (200), a value of 0.137 was calculated. Because these values are approximately the same, the ratio of the (210) has been taken as the α/β phase ratio. Attempts have also been made to analyse some of the data (Table 1) by Rietveld profile refinement (using the Philips crystallography program X'pert Plus) to obtain the weight fractions of each phase. Difficulties arose in performing a rigorous background correction, because of the considerable peak overlap and because the structures may be slightly different from those reported in Refs. [5–8]. Therefore, a range of best solutions is given, which are in a reasonable good agreement with the α fraction as derived from the ratio of the (210) reflections. From Table 1 it is confirmed that the ECO, EPCO(1.2) and the EHCO samples have the larges fraction of α crystals and in the order ECO > EPCO(1.2) > EHCO(2.3) > EHCO(4.8) > EPCO(2.9).

The width of the X-rays peaks (below 35°) was found to be approximately constant (0.5° 2θ) for all the samples implying that the crystallite size perpendicular to the polymer chain is about 200 Å. Some subtle differences were seen though between samples in the intensities of the $\{hk1\}$ reflections relative to those of the $\{hk0\}$ ones. For EBCO(4.7) the intensity of the $\{hk1\}$ reflections was high relative to that of the $\{hk0\}$s. This suggests better order along the polymer chain or alternatively a difference in orientation. However, subsequent work looking at differences between X-ray data collected in reflection and transmission only confirmed some orientation in sample EPCO(2.9). For all these samples, it was observed that the intensity of the $\{hk1\}$ reflections relative to the $\{hk0\}$ was substantially lower than those reported by Lommerts et al. [7] in drawn fibres and slightly lower than those given by Chatany [5]. This difference is probably mainly caused by drawing but there could be a small difference related to perfection along the chain.

A previous study carried out on ex-reactor aliphatic polyketones using Raman spectroscopy showed the potential of this technique for the elucidation of the physical and chemical structure of this family of materials [10]. Different Raman bands seen in the $-CH_2-$ bending vibrational range of different materials, were assigned to the α and β crystalline polymorphs proposed in the literature and discussed earlier (see Fig. 3). The presence of a band at 1440 cm^{-1} was assigned to the α form and is thought to arise from a factor group splitting effect in the orthorhombic lattice similar to that observed for other polymers, such as polyethylene, polyoxymethylene, etc. On the other hand, the presence of a band at 1430 cm^{-1} was attributed to the less packed distorted β form. This band was thought to arise from a weaker factor group splitting resulting in a smaller separation with the other component of the splitting, i.e. the band at 1415 cm^{-1}. This band at 1415 cm^{-1} is seen in all samples and it was tentatively assigned to the other component of the splitting for both polymorphs. Though this band is slightly shifted towards higher wavenumber in samples with β form, as a consequence of the reduction in interchain interaction induced by higher lattice volume. This band at ca. 1415 cm^{-1} is, therefore, common to both splittings. Some materials showed the three bands pointing to a crystal phase mixture of both structures. A more detailed discussion of this spectroscopic phenomenon seen in the $-CH_2-$ bending region and of the quantitative structural information that it can gathered in terms of crystalline polymorphism and crystalline density for aliphatic polyketones is drawn in Refs. [10,11].

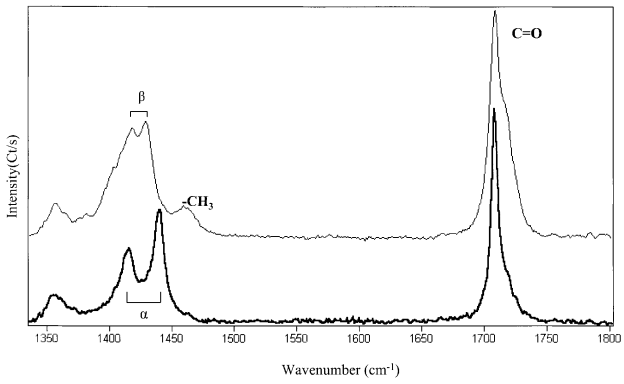

Fig. 3. Raman spectra in the range 1350–1750 cm^{-1} of (top) a sample with β form crystallinity and (bottom) of a material with α form crystallinity.

A number of ex-reactor powder polyketone samples namely, i.e. ECO, EPCO(5.1), EBCO(4.8) and EHCO(4.8) materials, were measured by Raman spectroscopy (see Fig. 4). By considering the above band assignments, it can be seen that the ex-reactor ECO and EHCO samples show a higher α-rich crystalline phase, i.e. higher presence of α crystals, whereas the EPCO polymer and, to a lesser extent the EBCO polymer, show a β-rich crystalline phase with a very low/absent and low pressure of α phase, respectively. Thus, for a relatively high second olefin incorporation

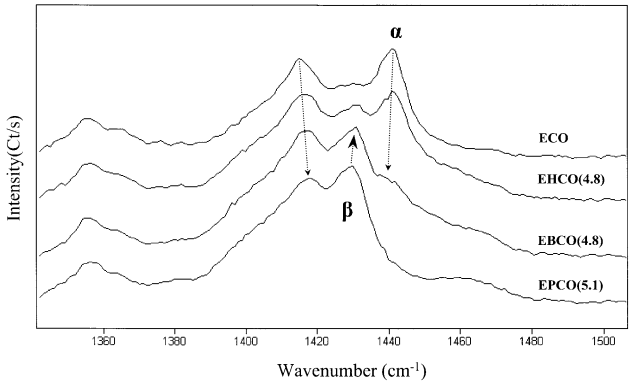

Fig. 4. Raman spectra in the range 1350–1530 cm^{-1} of, from top to bottom, ex-reactor ECO, EHCO(4.8), EBCO(4.8), EPCO(5.1).

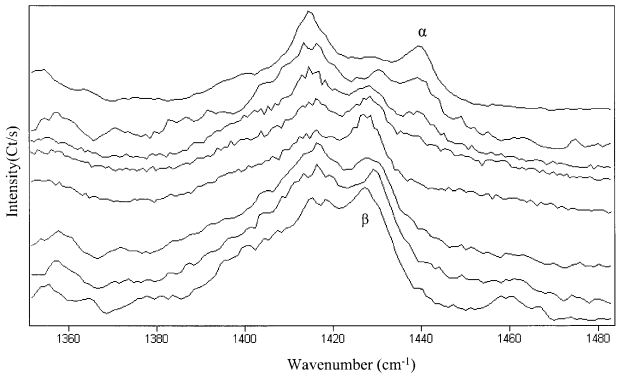

Fig. 5. Raman spectra in the range 1350–1530 cm^{-1} of, from top to bottom, ECO, EPCO(1.2), EHCO(2.3), EHCO(4.8), EBCO(4.8), EPCO(2.9), EPCO(5.1), EPCO(7.2).

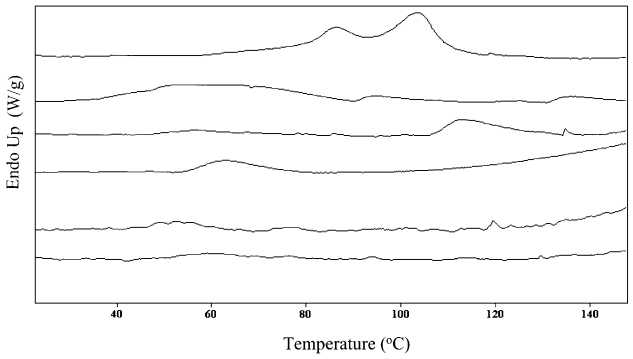

Fig. 6. DSC endotherms between 20 and 130 °C (phase transition range) of, from top to bottom, ECO, EPCO(1.2), EHCO(2.3), EHCO(4.8), and EBCO(4.8) and EPCO(5.1).

(resulting in branching) the ranking of α phase produced is in the order ECO > EHCO > EBCO > EPCO.

The Raman spectra of the compression moulded films, used for the WAXS measurements, are shown in the range of interest in Fig. 5. It is a general observation that compression moulding of the ex-reactor material results in a reduction of the original α phase present in the powder form (compare Figs. 4 and 5). Fig. 5 shows that the band at 1440 cm^{-1}, assigned to the α crystals, shows higher intensity for the ECO, EPCO(1.2) and EHCO samples, and in the order ECO > EPCO(1.2) > EHCO(2.3) > EHCO(4.8) > EPCO(2.9). Furthermore, this band is very weak or absent for the EBCO polymer and for the EPCO polymers with higher propene contents. Consequently, the Raman ranking of the α phase is seen qualitatively similar to that measured by WAXS (see Fig. 2).

Some of the samples were also scanned on heating by DSC. Upon heating a solid–solid phase transformation from α to β is thought to be triggered at around 100 °C. The β phase is the favoured phase for the polyketone crystals prior to melting. This temperature-induced phase change was unambiguously proved by Raman spectroscopy [10]. Fig. 6 displays the DSC heating endotherms of a number of polyketone samples. From the top curve in the figure, two clear endotherms peaked at 85 and 105 °C can be seen for the ECO sample. Some smaller endotherms can also be detected at different temperatures for the samples EPCO(1.2), EHCO(2.3) and EHCO(4.8). On the other hand, in the EBCO(4.8) and EPCO(5.1) samples, the endotherms are smaller or hardly discerned over a noisier baseline. The solid–solid phase change enthalpies were measured from the DSC runs of the samples that showed clear endotherms, and are gathered in Table 1. From the latter values, the phase change enthalpy for a perfect α crystal can be estimated using as input the α phase content measured by WAXS. This value is measured to be 32 ± 3 J g^{-1}. The error was found to be higher in the case of the sample EHCO(4.8) due to the very low content in α phase present in this sample. From Fig. 6, the EPCO(1.2) and EHCO(4.8) samples show the phase change endotherms at around 60 °C and above. The presence of transition peaks at, or from, lower temperature for these materials could be associated with lower crystal thickness and, to explain the multiplicity, with a distribution of α phase crystal sizes. As the phase change enthalpy for a perfect crystal is found to be rather constant across composition, at least for samples with α phase content higher that this in sample EHCO(4.8), the perfection of the α phase crystals must be similar among the different samples. The EBCO(4.8) and the corresponding EPCO(5.1) sample did not show such a clear α–β transition, in agreement with the very small/absent presence of α crystals measured by WAXS and Raman. From the above experiments, it can be deduced that all polyketone samples may have, to a higher or lower extent, α crystals as this is the most effective packing lattice in terms of maximizing the dipolar interchain interactions for this polymer; however, the presence of this α phase tends to be low, undetectable or absent in EPCO and EBCO polymers with relatively high levels of second olefin incorporation. For comparable levels of second olefin incorporation EBCO polymers exhibit somewhat higher proportion of α crystals than EPCO polymers (see Fig. 4).

3.2. Crystalline density by WAXS

The crystalline density of the dominant β phase present in the aliphatic polyketone samples studied here together with that from a number of other samples measured earlier at BP Chemicals laboratories with different contents and types of second olefin are plotted in Fig. 7. The crystalline density (using six reflections) of the α phase was only attempted for the ECO polymer because this sample showed the greatest proportion of this phase. This gives a value of $1.453(\pm 0.005)$ gr cm^{-3}. Earlier work showed that the decrease in crystalline density exhibited by aliphatic polyketones is mainly due to the enlargement of the *a* unit cell parameter [11]. Fig. 7 shows that the crystalline density tends to decrease with increasing comonomer content for EPCO and EBCO materials, whereas it stays rather constant for EHCO materials in the composition ranges studied. At a

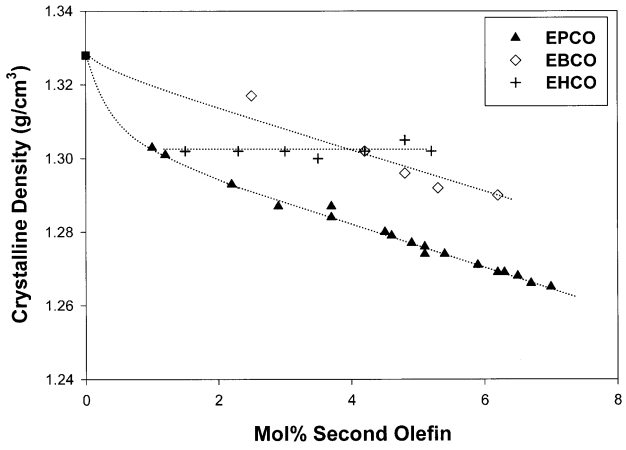

Fig. 7. Crystalline density as a function of second olefin content for a number of aliphatic polyketone materials as determined by WAXS experiments.

comparable second olefin concentration, EBCO polymers show higher crystalline density than EPCO polymers. The latter polymers clearly show two regimens in crystalline density namely, a rapid exponential-like decay with increasing propene content up to about 3 mol%, followed by a linear decrease upon further incorporation. This indicates that introduction of the first methyl branches has the largest impact on the crystalline density of the β phase. Unfortunately, sufficiently low second olefin concentration polymers are not available in the case of butene and hexene polymers. Nevertheless, it seems that the effect of introducing few ethyl branches in EBCO polymer has a more gentle impact on the density of the β phase crystals present. EHCO polymers are clearly different though, their β phase crystal density does not vary with composition across the composition range studied. The constant crystalline density seen for these polymers is higher than that of EPCO polymers with propene contents above 1 mol% and lower that EBCO polymers with butene contents below 4.5 mol%. The rough separation (in cm^{-1}) between the two components (1440–1415 cm^{-1}) of the Raman $-CH_2-$ bending factor group splitting for the α phase (estimated by curve-fitting of the Raman data as explained in Refs. [10,11]) is also given in Table 1. From this, it is seen that the splitting separation appears to decrease slightly in the order ECO > EHCO(2.3) ≅ EPCO(1.2) > EHCO(4.8). This effect can be also qualitatively observed in Figs. 4 and 5. As the reduction in the splitting separation is associated [11] with an increase in lattice volume, it could be that the crystalline density of the α phase is being reduced somewhat in the cited order. It should be borne in mind that the content in α phase determined by WAXS and Raman was found lower in EPCO and EBCO polymers and higher in EHCO polymers. These results can now be explained by realizing that as the concentration of branches rises, the chain sequences in EPCO and EBCO crystals are accommodated into a progressive more defective and thus lower crystalline density β phase. At this stage, it is worth noting that the true crystalline density of EPCO and EBCO materials cannot be accurately determined as we assumed for the calculations of the crystalline densities shown in Fig. 7 that only ECO (branch-free) chain segments build into the crystals. These results could be given as unit cell volumes but have been given as densities for ease of comparison with other published work.

3.3. Crystallinity

The heat of fusion and the crystallinity as determined by DSC and WAXS, respectively, of a number of polyketones samples are shown in Fig. 8. The heat of fusion was determined by integration of the endotherms seen from around 30 °C, and therefore includes the solid–solid phase change transition peaks, up to the end of melting. The heat of fusion clearly varies with the type of second olefin incorporated (see Fig. 8a). Thus, this is generally found to decrease (though not linearly) with increasing second olefin content, but for the same level of incorporation the heat of fusion decreases in the order EPCO > EHCO > EBCO. Fig. 8b

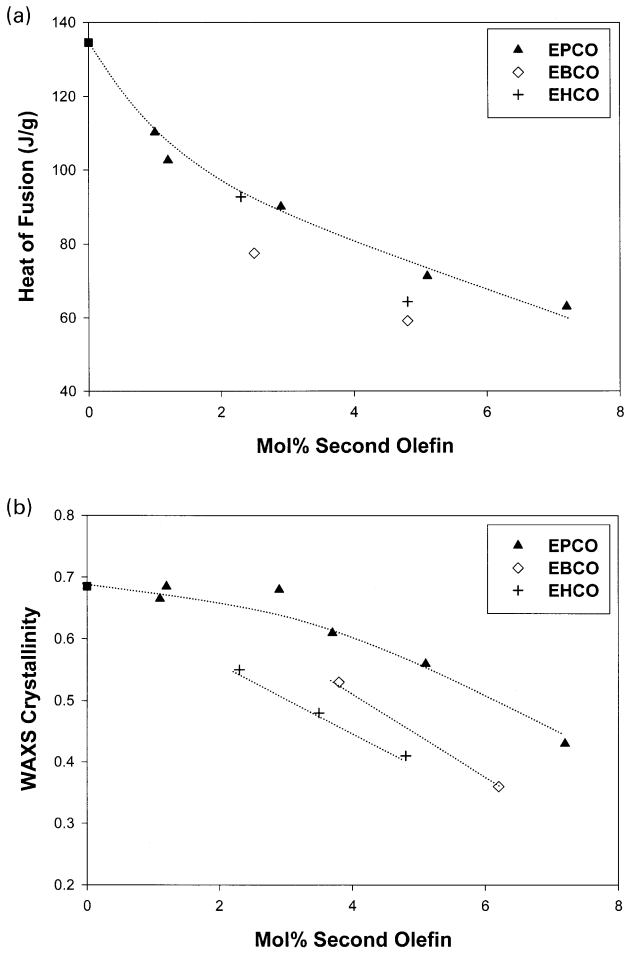

Fig. 8. (a) Heat of fusion as determined by DSC and (b) WAXS crystallinity as a function of second olefin content for a number of aliphatic polyketone materials.

shows the WAXS crystallinity as a function of second olefin concentration and type. From this figure, the crystallinity also decreases with increasing second olefin concentration but differently with respect to the heat of fusion, i.e. in the order EPCO > EBCO > EHCO. The crystallinity of EHCO polymers is found to decrease more rapidly than that of EBCO and EPCO polymers, and in addition EPCO polymers are more crystalline than EBCO polymers. Interestingly, the decrease in WAXS crystallinity for the EPCO polymers appears to be arrested at low second olefin concentration, whereas the heat of fusion was seen to decrease more rapidly in the same range. It is worthwhile noting that the film of the sample EPCO(2.9) measured by WAXS was found to be slightly oriented. Therefore, its crystallinity could be somewhat overestimated, hence the scatter in Fig. 8 for this sample. Although, no polymers of sufficiently low butene and hexene concentration are available to compare the crystallinity behaviour, by extrapolation to lower contents it would appear as if hexene polymers showed a tendency to decrease crystallinity in a more progressive and rapid manner across composition than propene and butene polymers. The discrepancy between the WAXS crystallinity and the DSC heat of fusion is quite marked for hexene polymers and for low second olefin content EPCO polymers, i.e. for polymers with higher α phase content and higher β phase crystalline density. In order to shed light into the cause of this discrepancy, the heat of fusion for a perfect polyketone crystal was also calculated using as input the WAXS crystallinity (see Table 1). From this table, it can be observed that far from being a constant value, the heat of fusion for a perfect crystal varies across second olefin type and content. Thus, this is higher for the ECO polymer and decreases with increasing propene concentration in EPCO polymers and for a similar concentration of side chains, this decreases in the order EHCO > EBCO > EPCO. Therefore, it is higher for those polymers having higher content of α phase and crystalline density. As a consequence, the heat of fusion for aliphatic polyketones appears to be not only a result of the mass fraction of crystals but must also be affected by the change in crystal morphology and crystal density across composition. Therefore, a more accurate reading of the crystallinity level present in these materials is thought to be given by WAXS measurements. From the WAXS crystallinity results, it can be concluded that (i) a low branch concentration is less effective in reducing crystallinity for at least polymers with methyl branches, and that (ii) longer branches have a larger effect on reducing crystallinity. The higher crystallinity observed for EPCO polymers at equal concentration of branches can be understood once one realize that these materials are capable of packing more chain sequences into crystals of lower crystalline density, i.e. ease of accommodating defects into crystals. Similarly, the lower crystallinity exhibited by hexene polymers arises from inability of these polymers to accommodate defects in their crystals deduced from the high content

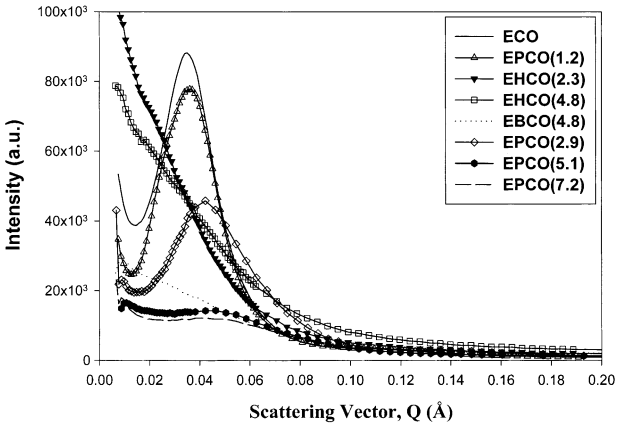

Fig. 9. SAXS curves of samples ECO, EPCO(1.2), EHCO(2.3), EHCO(4.8), EBCO(4.8), EPCO(2.9), EPCO(5.1), EPCO(7.2).

of α phase and the relatively high and constant crystalline density of the β phase observed for these polymers.

Fig. 9 and Table 2 show the SAXS curves and the resulting long period repeats of the samples, respectively. The long period was determined by two different methods. Both methods showed similar trends although the numerical results were slightly different, as has been reported before [17]. The branch-free sample, ECO, gave the clearest peak with a long period repeat of about 148 Å. As might be expected with increasing the concentration of propene the interference peak got weaker, broader and moved to higher scattering vectors, which implies smaller repeat distances. Moreover, as the peaks become broader there is an increasing range of repeat sizes, consequently the values given are a weighted average. For samples containing butene or hexene no interference peak was observed. EHCO polymers showed no indication of a repeat structure and in the EBCO(4.8) sample a weak peak was only just observable in the correlation function. By assuming a simple two-phase system comprising amorphous and crystalline phases with sharp boundaries, an estimation of the average crystal thickness (L_c) was obtained (see Table 1). Table 2 also gives the calculated theoretical distance

Table 2
SAXS long period repeats (estimated error ±5 Å) as determined from the maximum in the desmeared Lorentz corrected data (L_1) and from the maximum in the one dimensional correlation function (L_2), the corresponding crystal thickness and estimated average size of crystallisable sequences free of branches along the polyketone chain

Sample	L_1 (Å)	L_2 (Å)	L_{c1} (Å)	L_{c2} (Å)	$L_{branch\text{-}free}$ (Å)
ECO	148	138	101	94	–
EPCO(1.2)	142	135	97	92	134
EPCO(2.9)	108	100	73	68	53
EPCO(5.1)	100	90	56	50	29
EPCO(7.2)	90	90	39	39	19
EBCO(4.8)	–	110	–	40	31
EHCO(2.3)	–	–	–	–	–
EHCO(4.8)	–	–	–	–	–

between branch-free crystallizable (given the fact that the *c* axis of the lattice is unaffected across composition, i.e. $c = 7.60$ Å) sequences for a perfectly homogenous incorporation of the branches along the polyketone chain. By comparison of the latter distance with the average crystal thickness, we can observed that the size of the crystal in the *c* direction tends in all samples, except in EPCO(1.2), to be larger. This observation may indeed support, together with the above results of crystalline density and α phase content, the argument that inclusion of branches in the crystals must occur in EPCO and presumably in EBCO polymers. The fact that the crystallinity appears to decrease at a lower pace in EPCO polymers with low levels of second olefin may also be indicative of branches building in the crystals. The above SAXS results are therefore consistent with the results from other techniques. If the side chains in EHCO are always rejected from the crystalline regions, the crystalline regions are more perfect but cannot build up into an ordered lamellar repeat structure. However, with some side chain incorporation EPCO samples can give a rather disordered repeat structure at high levels of second olefin. The drop in crystalline density reduces the crystalline amorphous contrast and is a contributory factor in reducing the intensity. The intensity is also reduced by other imperfections in the repeating structure caused by the side chains that are rejected. Behaviour of the EBCO polymer is intermediate between that of the EPCO and the EHCO materials.

3.4. Melting behaviour

The melting point (maximum of melting) and the endset of melting (defined as the intercept between the fall of the melting peak and the baseline) are plotted as functions of the second olefin incorporation in Fig. 10. From this Fig. 10, it can be observed that both temperatures clearly decrease with increasing second olefin content. Nevertheless, while the maximum of melting (Fig. 10a) for all polymers seems to largely fit to a single compositional line with some scatter for low second olefin content EHCO polymers, the endset of melting (Fig. 10b) is clearly higher for hexene polymers while decreases seemingly (though no linearly) for the other two types. Fig. 11 shows some of the DSC traces. From those, it is seen that the melting behaviour is very complex in aliphatic polyketones; thus, and as reported earlier [7,8], it tends to be broad and multiple for most of the samples, especially for the EHCO sample in Fig. 11. In this sample two largely separated melting features, one rather broad and the other sharp, can be seen, hence the two points plotted in Fig. 10a to represent this material. It is therefore not surprising that these polymers do not give a defined interference peak in their SAXS data.

The above melting point behaviour is rather surprising, since in analogous random ethylene copolymers the melting point has been reported to behave differently across composition [18,19]. Thus, the melting point of ethylene–propene copolymers (resulting in methyl side chains, and therefore

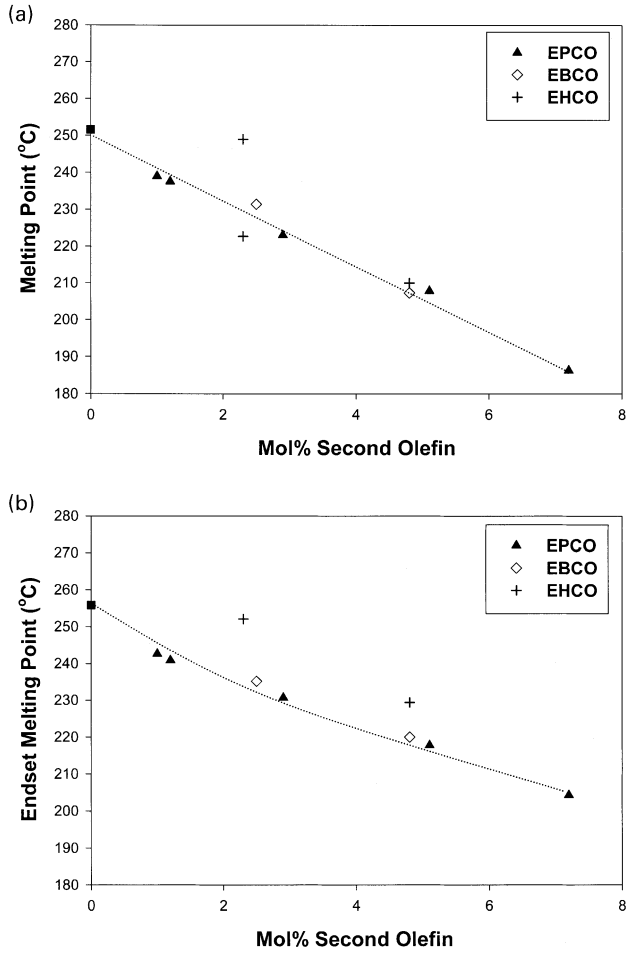

Fig. 10. (a) Melting point (maximum of melting) and (b) Endset of melting as a function of second olefin content for a number of aliphatic polyketone materials as determined by DSC experiments.

analogous to EPCO polymers in terms of branches) has repeatedly been found unambiguously higher that that of corresponding copolymers of ethylene and 1-olefins of longer chain length. In the case of the latter ethylene copolymers, i.e. ethylene-1-olefin copolymers where the 1-olefin is longer than propene, the melting point is found

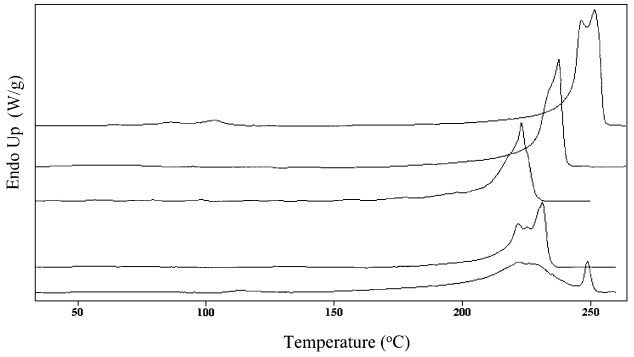

Fig. 11. DSC traces of, from top to bottom, ECO, EPCO(1.2), EPCO(2.9), EBCO(2.5) and EHCO(2.3).

however to be independent of branch length, at least for low comonomer contents. When some dependency has been experimentally found between the latter range of copolymers, this has been mainly ascribed to molecular heterogeneity [16]. Significant molecular heterogeneity for polyketone polymers would be surprising because of these polymers are known to be highly random [1–4]. A general thermodynamic theory developed by Flory revealed that random copolymers are expected to decrease their melting point with respect to that of the homopolymer as the branch concentration increases [20]. This theory assumes that co-unit does not enter the lattice. In ethylene copolymers however, the melting point does decrease more steeply than predicted by the theory [18]. The discrepancy between theory and experimental is ascribed to (I) the difficulty in crystallizing a sufficient concentration of very long sequences that are required to satisfy equilibrium conditions, (II) the incorporation of the side chain in the crystals, (III) the presence of very thin lamella, (IV) dilatometric stresses at the interface due to the reduced lamella thickness, etc. Furthermore, the interpretation of melting of branched polymers can be complicated by phenomena such as annealing, rearrangements (solid–solid phase transformation), multiple melting points (a pattern in aliphatic polyketones, see Fig. 11) and recrystallization of poor crystals.

From Fig. 10b, it is observed that by linear extrapolation of the endset melting points of the EHCO materials a value of 273 °C is reached at the intercept with the Y axis. This temperature is very close to that measured [7] at 278 °C in a highly drawn ECO branch-free polymer, which was assumed to be a good approximation of the actual equilibrium temperature, T_m^0. The endset represents the temperature at which the last crystalline traces of the sample melt, therefore corresponds to the melting temperature of the most stable, annealed and/or recrystallized and closer to thermodynamic equilibrium crystals. The equilibrium theory for a random copolymer in which the side chains do not enter the crystals as proposed by Flory [21,22] can be expressed by the following equation

$$\frac{1}{T_m} - \frac{1}{T_m^0} = -\frac{R}{H_f} \ln X$$

where T_m is the copolymer melting point, T_m^0 is the homopolymer melting point ($T_m^0 = 278$ °C from Ref. [7]), H_f is the enthalpy of fusion per repeating unit (H_f was estimated to be between 4 and 6.2 kJ mol^{-1} from Ref. [7]) and X is the mole fraction of crystallizing units. By inputting the EHCO endset melting point data and solving this equation for H_f a value of 4.5 kJ mol^{-1} (245 J g^{-1}) is obtained. This is indeed within the range, 4–6.2 kJ mol^{-1}, of heat of fusion for a perfect crystal reported in Ref. [7], suggesting that the hexene polymers could be the closest polyketone polymers to be described by the exclusion argument imposed by the Flory equation. It is worthwhile noting though, that as the vast majority of crystals present in a sample undergo melting at lower temperatures than the endset, it is clear from comparing Fig. 10a and b that none of the samples with melting point represented by the maximum of melting, will follow the equilibrium trend in the composition range studied here. The reasons for the discrepancy between experimental and theory have been outlined before. A value of H_f at 245 J g^{-1} is indeed much higher that those gathered in Table 1 and derived from DSC and WAXS data of the samples studied here. It is also surprising to observe the large discrepancy between the melting point temperature measured for the compression moulded ECO material, i.e. ca. 252 °C, used in this study and that at 278 °C of a highly drawn branch-free polyketone fibre. As the main difference between both materials is the content in α phase, exclusive for the drawn fibre, and in spite of the solid–solid phase change at around 100 °C, the melting point seems to be strongly influenced, albeit not only, by the original α/β ratio phase content. As a result of all the above, much caution should be taken when interpreting the melting behaviour of these polymers.

4. Discussion and concluding remarks

Now it is convenient to sum up the results to provide a feasible picture of the effects that the size of the second olefin (which gives side chains) induce in the polyketones crystalline morphology. WAXS, Raman and DSC data show that ECO and EHCO polymers do contain a higher fraction of the denser α crystalline phase. This polymorph leads indeed to the most effective packing that maximizes the dipolar interchain interaction, for the polyketone chains in the ordered phase. However, EBCO polymers and particularly EPCO polymers exhibit higher crystallinity and favour the less dense β phase. As the latter polymers crystallize with more impediments or defects their chains cannot pack into the denser α phase. In addition, it is found that the crystalline density of the β phase present in the different materials also varies. The crystalline density is calculated from the unit cell volume and thus relates to the health of the crystals in terms of defects or impediments. EPCO polymers exhibit a more ill-defined crystal structure, therefore, the presence of internal defects appears evident. This was already suggested by Klop et al. [8] for EPCO polymers.

The incorporation of the small methyl branches as defects into the crystals must be a feasible explanation for inability of this polymer to effectively pack the chains into the denser lattices. Methyl branches, although still the subject of some discussion, are widely accepted as being capable of building into ethylene–propene copolymer crystals [18,19]. Some debate remains also open as to whether longer branches, such as ethyl side chains, can be accommodated in the crystals or are segregated to the disordered amorphous phase. The lack of melting point dependence with the comonomer size in ethylene copolymer (with 1-olefins longer than propene) strongly suggests that ethyl and longer branches are likely to remain outside the crystals. In polyketones,

EBCO polymers do show higher crystalline density than EPCO polymers, indicating that ethyl branches are not as likely as methyl branches to build into the crystals, but the crystalline density is also seen to decrease across composition. Furthermore, as EBCO polymers exhibit a closer behaviour in terms of polymorphism, melting point, and average crystal thickness vs. branch-free crystallizable chain sequences distance and crystallinity to EPCO polymers some inclusion must also be regarded. EHCO polymers are definitely different polymers than the latter two types. The presence of larger number of crystals, a constant crystalline density across composition for the β phase, lower crystallinity, and higher endset melting temperatures falling within the equilibrium range clearly support the exclusion argument for these polymers. The EHCO polymers must develop β phase crystals of a relatively high and constant crystalline density at expenses of the α phase as the branching content increases. However, a point should be reached where the lamella becoming thinner will reduce the crystalline density. Unit cell expansion, i.e. crystalline density drop, is also thought to originate from lamella thickness reduction due to surface dilatometric stresses, thermal vibrations and intracrystalline defects resulting form faster crystallization at the large undercoolings required [23]. The cited regime does definitely not affect the β phase in the range of second olefin concentration studied here because (i) some α phase is still present and (ii) the crystalline density is seen constant across the composition range. However, the above effect, i.e. lamella becoming thinner, must cause the progressive change of α crystals into high crystalline density β ones as the second olefin concentration is increased in EHCO polymers. Nonetheless, the drop in crystalline density observed for EPCO and also for EBCO polymers is not likely to be originated from the latter effect because the crystalline density for these materials is in general below the constant value exhibited by the EHCO materials; therefore, it must originate to a greater extent from the incorporation of some branches as defects in the crystals. The depression at a lower pace of the crystalline density for polymers with concentrations of propene above 3 mol% could be related to the more rapid crystallinity depression observed for these propene samples. The latter behaviour could be attributed to branches rejected from the crystallites into the amorphous phase as the concentration of propene increases, hence hindering more effectively crystallization.

Two possible reasons why ethyl branches should be more likely to build into polyketone crystals than in polyethylene crystals proposed: (i) the cross-sectional area of the unit cell (ab) of beta phase polyketone is somewhat larger (~37.5 $Å^2$) than that of polyethylene (~36.5 $Å^2$) and so there is more room to accommodate a side chain; (ii) the degree of self-association (cohesive energy) is very high in aliphatic polyketones due to the interchain dipolar interaction induced by the perfectly alternating network of carbonyl groups. Consequently, highly stable lateral cohesive packing can be achieved, which may compensate the free energy excess associated with the accommodation of defects.

Acknowledgements

The authors would like to thank Dr N.M. Dixon (BP Chemicals) for the Raman measurements and to Mr P. Daniell (BP Chemicals) for supplying samples and valuable characterisation data. BP Chemicals is acknowledged for granting permission to publish this work.

References

[1] Drent E, Budzelaar PHM. Chem Rev 1996;96:633.
[2] Sommazzi A, Garbassi F. Prog Polym Sci 1997;22:1547.
[3] Bonner JG, Powell AK. 213th National American Chemical Society Meeting. Washington: ACS Materials Chemistry Publications, 1997.
[4] Bonner JG, Powell AK. New Plastics'98 Conference Proceedings. London: CSIR, 1998.
[5] Chatany Y, Takizawa T, Murahashi S, Sakata Y, Nishmura Y. J Polym Sci 1961;55:811.
[6] Chatany Y, Takizawa T, Murahashi S. J Polym Sci 1962;62:S27.
[7] Lommerts BJ, Klop EA, Aerts J. J Polym Sci Polym Phys 1993;31:1319.
[8] Klop EA, Lommerts BJ, Veurink J, Aerts J, Van Puijenbroek RR. J Polym Sci Polym Phys 1995;33:315.
[9] Waddon AJ, Karttunen NR. Polymer 2001;42:2039.
[10] Lagaron JM, Powell AK, Davidson NS, Dixon NM. Macromolecules 2000;33:1030.
[11] Lagaron JM, Vickers ME, Powell AK, Bonner JG. Polymer 2000;41:3011.
[12] Mason SM, Conroy N, Dixon NM, Williams KPJ. Spectrochim Acta 1993;49a:633.
[13] Langford JI, Louer D, Sonneveld EJ, Visser JW. Powder Diffraction 1986;1:211.
[14] Balta-Calleja FJ, Vonk CG. X-ray scattering of synthetic polymers. Amsterdam: Elsevier, 1989.
[15] Wilson ACJ. J Sci Instrum 1950;27:321.
[16] Vonk CG. J Appl Crystallogr 1975;8:340.
[17] Blundell DJ. Polymer 1978;19:1258.
[18] Alamo R, Domszy R, Mandelkern L. J Phys Chem 1984;88:6587.
[19] Clas S-D, Mcfaddin DC, Russell KE, Scmmel-Bullock MV. J Polym Sci Polym Chem 1987;25:3105.
[20] Mandelkern L. Crystallization of polymers. New York: McGraw-Hill, 1964. p. 74.
[21] Flory PJ. J Chem Phys 1949;17:223.
[22] Flory PJ. Trans Faraday Soc 1995;51:848.
[23] Howard PR, Crist B. J Polym Sci Phys 1989;27:2269.